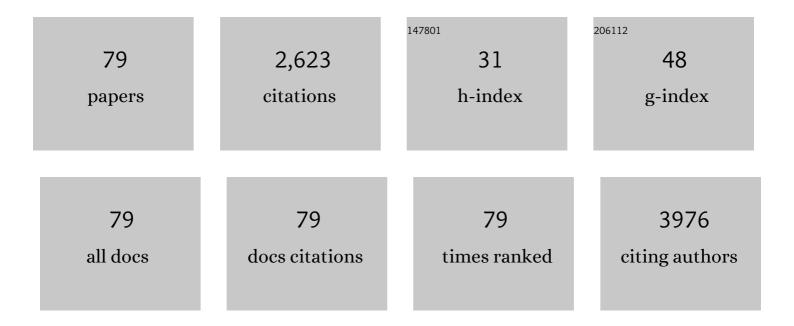
List of Publications by Year in descending order

Source: https://exaly.com/author-pdf/6044445/publications.pdf

Version: 2024-02-01



Υονς Ζηγνς

#	Article	IF	CITATIONS
1	Hydrothermal synthesis of layered molybdenum sulfide/N-doped graphene hybrid with enhanced supercapacitor performance. Carbon, 2016, 99, 35-42.	10.3	183
2	A facile synthesis of mesoporous Co ₃ O ₄ /CeO ₂ hybrid nanowire arrays for high performance supercapacitors. Journal of Materials Chemistry A, 2015, 3, 10425-10431.	10.3	108
3	MOF-74 derived porous hybrid metal oxide hollow nanowires for high-performance electrochemical energy storage. Journal of Materials Chemistry A, 2018, 6, 8396-8404.	10.3	101
4	A solvent-assisted ligand exchange approach enables metal-organic frameworks with diverse and complex architectures. Nature Communications, 2020, 11, 927.	12.8	93
5	Cryo-mediated exfoliation and fracturing of layered materials into 2D quantum dots. Science Advances, 2017, 3, e1701500.	10.3	91
6	CeO _{2â^'x} /C/rGO nanocomposites derived from Ce-MOF and graphene oxide as a robust platform for highly sensitive uric acid detection. Nanoscale, 2018, 10, 1939-1945.	5.6	88
7	Z-scheme carbon-bridged Bi2O3/TiO2 nanotube arrays to boost photoelectrochemical detection performance. Applied Catalysis B: Environmental, 2019, 248, 255-263.	20.2	85
8	Tungsten oxide nanowires grown on carbon paper as Pt electrocatalyst support for high performance proton exchange membrane fuel cells. Journal of Power Sources, 2009, 192, 330-335.	7.8	84
9	3D Coral-Like Ni ₃ S ₂ on Ni Foam as a Bifunctional Electrocatalyst for Overall Water Splitting. ACS Applied Materials & Interfaces, 2018, 10, 31330-31339.	8.0	80
10	Designed growth of WO3/PEDOT core/shell hybrid nanorod arrays with modulated electrochromic properties. Chemical Engineering Journal, 2019, 355, 942-951.	12.7	72
11	A high performance electrochemical biosensor based on Cu ₂ O–carbon dots for selective and sensitive determination of dopamine in human serum. RSC Advances, 2015, 5, 54102-54108.	3.6	68
12	Size-dependent surface phase change of lithium iron phosphate during carbon coating. Nature Communications, 2014, 5, 3415.	12.8	66
13	Chromate cathode decorated with in-situ growth of copper nanocatalyst for high temperature carbon dioxide electrolysis. International Journal of Hydrogen Energy, 2014, 39, 20888-20897.	7.1	54
14	Water-Soluble Defect-Rich MoS ₂ Ultrathin Nanosheets for Enhanced Hydrogen Evolution. Journal of Physical Chemistry Letters, 2019, 10, 3282-3289.	4.6	50
15	Synthesis and electrochemical properties of LSM and LSF perovskites as anode materials for high temperature steam electrolysis. Journal of Power Sources, 2009, 186, 485-489.	7.8	49
16	Three-Dimensional Hierarchical Structure of Single Crystalline Tungsten Oxide Nanowires: Construction, Phase Transition, and Voltammetric Behavior. Journal of Physical Chemistry C, 2009, 113, 1746-1750.	3.1	49
17	Construction of CuO/Cu2O@CoO core shell nanowire arrays for high-performance supercapacitors. Surface and Coatings Technology, 2016, 299, 15-21.	4.8	49
18	Reversibly in-situ anchoring copper nanocatalyst inÂperovskite titanate cathode for direct high-temperature steam electrolysis. International Journal of Hydrogen Energy, 2014, 39, 5485-5496.	7.1	48

#	Article	IF	CITATIONS
19	Enhanced photocatalytic performances of ultrafine g-C3N4 nanosheets obtained by gaseous stripping with wet nitrogen. Applied Surface Science, 2018, 427, 730-738.	6.1	47
20	Rational Design of Oxygen Deficiency-Controlled Tungsten Oxide Electrochromic Films with an Exceptional Memory Effect. ACS Applied Materials & Interfaces, 2020, 12, 32658-32665.	8.0	46
21	Structure modulated amorphous/crystalline WO3 nanoporous arrays with superior electrochromic energy storage performance. Solar Energy Materials and Solar Cells, 2020, 212, 110579.	6.2	45
22	Crystalline WO3 nanowires array sheathed with sputtered amorphous shells for enhanced electrochromic performance. Applied Surface Science, 2019, 498, 143796.	6.1	42
23	Synthesis of porous NiO/CeO ₂ hybrid nanoflake arrays as a platform for electrochemical biosensing. Nanoscale, 2016, 8, 770-774.	5.6	41
24	<i>In situ</i> growth of PEDOT/graphene oxide nanostructures with enhanced electrochromic performance. RSC Advances, 2018, 8, 13679-13685.	3.6	41
25	3D boron doped carbon nanorods/carbon-microfiber hybrid composites: synthesis and applications in a highly stable proton exchange membrane fuel cell. Journal of Materials Chemistry, 2011, 21, 18195.	6.7	38
26	MoS2 quantum dots decorated ultrathin NiO nanosheets for overall water splitting. Journal of Colloid and Interface Science, 2020, 566, 411-418.	9.4	38
27	Ultrathin carbon coated mesoporous Ni-NiFe2O4 nanosheet arrays for efficient overall water splitting. Electrochimica Acta, 2019, 321, 134652.	5.2	37
28	3D carbon coated NiCo2S4 nanowires doped with nitrogen for electrochemical energy storage and conversion. Journal of Colloid and Interface Science, 2019, 556, 449-457.	9.4	37
29	Size-Controlled TiO 2 nanocrystals with exposed {001} and {101} facets strongly linking to graphene oxide via p -Phenylenediamine for efficient photocatalytic degradation of fulvic acids. Journal of Hazardous Materials, 2016, 314, 41-50.	12.4	35
30	Fabrication of WO3/TiO2 core-shell nanowire arrays: Structure design and high electrochromic performance. Electrochimica Acta, 2020, 330, 135189.	5.2	34
31	Carbon-coated tungsten oxide nanowires supported Pt nanoparticles for oxygen reduction. International Journal of Hydrogen Energy, 2012, 37, 4633-4638.	7.1	33
32	Preparation of V ₂ O ₅ dot-decorated WO ₃ nanorod arrays for high performance multi-color electrochromic devices. Journal of Materials Chemistry C, 2018, 6, 12206-12216.	5.5	31
33	Hierarchical NiCo2O4/MnO2 core–shell nanosheets arrays for flexible asymmetric supercapacitor. Journal of Materials Science, 2020, 55, 688-700.	3.7	31
34	Robust production of 2D quantum sheets from bulk layered materials. Materials Horizons, 2019, 6, 1416-1424.	12.2	28
35	PEDOT hollow nanospheres for integrated bifunctional electrochromic supercapacitors. Organic Electronics, 2020, 77, 105497.	2.6	28
36	Synthesis of α-Bi ₂ Mo ₃ O ₁₂ /TiO ₂ Nanotube Arrays for Photoelectrochemical COD Detection Application. Langmuir, 2017, 33, 8933-8942.	3.5	27

#	Article	IF	CITATIONS
37	Single-phase nickel-doped ceria cathode with in situ grown nickel nanocatalyst for direct high-temperature carbon dioxide electrolysis. RSC Advances, 2014, 4, 40494-40504.	3.6	26
38	Carbon-Coated Self-Assembled Ultrathin T-Nb ₂ O ₅ Nanosheets for High-Rate Lithium-Ion Storage with Superior Cycling Stability. ACS Applied Energy Materials, 2020, 3, 12037-12045.	5.1	26
39	Nitrogen, sulfur-codoped micro–mesoporous carbon derived from boat-fruited sterculia seed for robust lithium–sulfur batteries. RSC Advances, 2019, 9, 15715-15726.	3.6	24
40	Self-assembly of 0D/2D homostructure for enhanced hydrogen evolution. Materials Today, 2020, 36, 83-90.	14.2	24
41	Controlled synthesis of MnO2@TiO2 hybrid nanotube arrays with enhanced oxygen evolutionÂreaction performance. International Journal of Hydrogen Energy, 2018, 43, 14369-14378.	7.1	22
42	Fabrication of CoFe/N-doped mesoporous carbon hybrids from Prussian blue analogous as high performance cathodes for lithium-sulfur batteries. International Journal of Hydrogen Energy, 2019, 44, 20257-20266.	7.1	20
43	Hydrothermal synthesis of well-standing δ-MnO2 nanoplatelets on nitrogen-doped reduced graphene oxide for high-performance supercapacitor. Journal of Alloys and Compounds, 2019, 787, 309-317.	5.5	19
44	In situ W/O Co-doped hollow carbon nitride tubular structures with enhanced visible-light-driven photocatalytic performance for hydrogen evolution. International Journal of Hydrogen Energy, 2021, 46, 234-246.	7.1	19
45	Integration of mesoporous nickel cobalt oxide nanosheets with ultrathin layer carbon wrapped TiO ₂ nanotube arrays for high-performance supercapacitors. New Journal of Chemistry, 2016, 40, 6881-6889.	2.8	18
46	Effect of conductive PANI vs. insulative PS shell coated Ni nanochains on electromagnetic wave absorption. Journal of Alloys and Compounds, 2020, 821, 153531.	5.5	18
47	Metal-organic framework-derived porous Cu2O/Cu@C core-shell nanowires and their application in uric acid biosensor. Applied Surface Science, 2020, 506, 144662.	6.1	18
48	Controlled Production of MoS ₂ Fullâ€Scale Nanosheets and Their Strong Size Effects. Advanced Materials Interfaces, 2020, 7, 2001130.	3.7	17
49	One-step electrodeposition of Co 0·12 Ni 1·88 S 2 @Co 8 S 9 nanoparticles on highly conductive TiO 2 nanotube arrays for battery-type electrodes with enhanced energy storage performance. Journal of Power Sources, 2017, 364, 400-409.	7.8	17
50	CoO Quantum Dots Anchored on Reduced Graphene Oxide Aerogels for Lithium-Ion Storage. ACS Applied Nano Materials, 2020, 3, 10369-10379.	5.0	16
51	Tuning Morphology and Electronic Structure of Amorphous NiFeB Nanosheets for Enhanced Electrocatalytic N ₂ Reduction. ACS Applied Energy Materials, 2020, 3, 9516-9522.	5.1	16
52	Synthesis of W2N nanorods-graphene hybrid structure with enhanced oxygen reduction reaction performance. International Journal of Hydrogen Energy, 2017, 42, 25924-25932.	7.1	14
53	Directly Exfoliated Ultrathin Silicon Nanosheets for Enhanced Photocatalytic Hydrogen Production. Journal of Physical Chemistry Letters, 2020, 11, 8668-8674.	4.6	14
54	A general strategy for semiconductor quantum dot production. Nanoscale, 2021, 13, 8004-8011.	5.6	13

#	Article	IF	CITATIONS
55	Graphene quantum dots interfacial-decorated hierarchical Ni/PS core/shell nanocapsules for tunable microwave absorption. Journal of Alloys and Compounds, 2020, 848, 156529.	5.5	12
56	Construction of three-dimensional hierarchical Pt/TiO2@C nanowires with enhanced methanol oxidation properties. International Journal of Hydrogen Energy, 2020, 45, 33440-33447.	7.1	12
57	Rational construction of porous amorphous WO3 nanostructures with high electrochromic energy storage performance: Effect of temperature. Journal of Non-Crystalline Solids, 2020, 549, 120337.	3.1	12
58	Designed Construction of SrTiO ₃ /SrSO ₄ /Pt Heterojunctions with Boosted Photocatalytic H ₂ Evolution Activity. Chemistry - A European Journal, 2021, 27, 7300-7306.	3.3	12
59	In-situ synthesis of carbon-coated β-NiS nanocrystals for hydrogen evolution reaction in both acidic and alkaline solution. International Journal of Hydrogen Energy, 2018, 43, 16061-16067.	7.1	11
60	Controlled growth of porous oxygen-deficient NiCo ₂ O ₄ nanobelts as high-efficiency electrocatalysts for oxygen evolution reaction. Catalysis Science and Technology, 2021, 11, 264-271.	4.1	11
61	Pseudocapacitive TiNb2O7/reduced graphene oxide nanocomposite for high–rate lithium ion hybrid capacitors. Journal of Colloid and Interface Science, 2022, 610, 385-394.	9.4	11
62	Supercapacitive performance of single phase CuO nanosheet arrays with ultra-long cycling stability. Journal of Alloys and Compounds, 2018, 753, 731-739.	5.5	10
63	Tailoring Multi-Walled Carbon Nanotubes into Graphene Quantum Sheets. ACS Applied Materials & Interfaces, 2020, 12, 47784-47791.	8.0	10
64	Synthesis of SrTiO ₃ submicron cubes with simultaneous and competitive photocatalytic activity for H ₂ O splitting and CO ₂ reduction. RSC Advances, 2020, 10, 42619-42627.	3.6	10
65	Scalable production of intrinsic WX ₂ (XÂ=ÂS, Se, Te) quantum sheets for efficient hydrogen evolution electrocatalysis. Nanotechnology, 2021, 32, 495701.	2.6	10
66	Designing core–shell metal–organic framework hybrids: toward high-efficiency electrochemical potassium storage. Journal of Materials Chemistry A, 2021, 9, 26181-26188.	10.3	10
67	A surface precleaning strategy intensifies the interface coupling of the Bi ₂ O ₃ /TiO ₂ heterostructure for enhanced photoelectrochemical detection properties. Materials Chemistry Frontiers, 2020, 4, 638-644.	5.9	9
68	Nanoporous carbon nanowires derived from one-dimensional metal-organic framework core-shell hybrids for enhanced electrochemical energy storage. Applied Surface Science, 2022, 576, 151800.	6.1	9
69	Carbon Nanolayer-Wrapped Mesoporous TiO ₂ –B/Anatase for Li ⁺ Storage. ACS Applied Nano Materials, 2021, 4, 7832-7839.	5.0	8
70	Construction of WO3/Ti-doped WO3 bi-layer nanopore arrays with superior electrochromic and capacitive performances. Tungsten, 2019, 1, 236-244.	4.8	7
71	Tunable Synthesis of 3D Niobium Oxynitride Nanosheets for Lithium-Ion Hybrid Capacitors with High Energy/Power Density. ACS Sustainable Chemistry and Engineering, 2021, 9, 14569-14578.	6.7	7
72	Ti ₃ AlC ₂ MAX and Ti ₃ C ₂ MXene Quantum Sheets for Record-High Optical Nonlinearity. Journal of Physical Chemistry Letters, 2022, 13, 3929-3936.	4.6	7

YONG ZHANG

#	Article	IF	CITATIONS
73	In-situ constructing hybrid oxygen electrode of porous Co3O4 nanowire array on La0.8Sr0.2MnO3â^´Î´ for steam electrolysis. International Journal of Hydrogen Energy, 2016, 41, 5428-5436.	7.1	6
74	Enhanced Oxygen Reduction Catalysis of Carbon Nanohybrids from Nitrogen-Rich Edges. Langmuir, 2020, 36, 13752-13758.	3.5	5
75	Enhanced Energy Storage Performance of 3D Hybrid Metal Sulfides via Synergistic Engineering of Architecture and Composition. ACS Sustainable Chemistry and Engineering, 2020, 8, 11491-11500.	6.7	5
76	In-situ constructing NiO nanoplatelets network on La 0.75 Sr 0.25 Mn 0.5 Cr 0.5 O 3-Î′ electrode with enhanced steam electrolysis. International Journal of Hydrogen Energy, 2017, 42, 5657-5666.	7.1	4
77	High-yielding preparation of hierarchically branched carbon nanotubes derived from zeolitic imidazolate frameworks for enhanced electrochemical K ⁺ storage. Dalton Transactions, 2022, 51, 5441-5447.	3.3	4
78	Hierarchical Hybrid of Few-Layer Graphene upon Tungsten Monocarbide Nanowires: Controlled Synthesis and Electrocatalytic Performance for Methanol Oxidation. ACS Applied Energy Materials, 2019, 2, 328-337.	5.1	3
79	In-situ construction of NiCo2O4 nanoarrays on La0.8Sr0.2MnO3-δ electrodes for intermediate temperature solid oxide fuel cells. Journal of Solid State Electrochemistry, 2018, 22, 2367-2374.	2.5	О